Penalty Design for Uniform Spatial Resolution in 3D Penalized-Likelihood Image Reconstruction

J. Webster Stayman and Jeffrey A. Fessler
4415 EECS Dept., University of Michigan, Ann Arbor, MI 48109
email: stayman@eecs.umich.edu

Abstract— The object-dependent space-variant smoothing properties of penalized-likelihood estimators using conventional space-invariant regularizations have been demonstrated in [1,2]. We have presented a technique in [3,4] which provides nearly space-invariant resolution properties for the two-dimensional case. This is accomplished through a modification of the penalty term in the penalized-likelihood objective function, and is based on least-squares fitting of a parameterized local impulse response to a desired global response. That technique is extended here for the fully three-dimensional case.

I. Introduction

Conventional space-invariant penalties for penalized-likelihood image reconstruction yield images with object-dependent nonuniform spatial resolution properties [1, 2]. For example, in emission tomography such estimators tend to smooth the image more in high count regions than in low count regions. In addition, if one views the local point spread functions (PSFs) [1, 5], the smoothing properties can be highly anisotropic. Anisotropic 3D PSFs mean that objects within an image are distorted nonuniformly. For example, a spherical objects may appear elliptical due to more blurring in one direction. (Such distortions are noticeable in reconstructions of phantom data in [3, 6] and have been noticed by colleagues in a clinical setting.)

We have demonstrated a technique that provides nearly space-invariant resolution properties in [3, 4] for tomographic systems operating in two-dimensional mode. This technique controls the resolution properties of the reconstructed image through a modified penalty term in the penalized-likelihood objective function. This penalty design is based on a parameterization of the penalty term, followed by the determination of penalty term coefficients. We determine these coefficients through a least-squares fitting of a parameterized local impulse response[1] to an arbitrary desired global shift-invariant response. In this paper, we extend our penalty design method to the fully three-dimensional case, using the 3D point spread function and a 3D penalty.

As in [3, 4], we are concerned with the resolution properties of penalized-likelihood estimators iterated until convergence, and an idealized tomographic system whose intrinsic geometric response is nearly space-invariant. In this context, spatial resolution nonuniformity is due to the objective function, *not* the system geometry.

This work was supported in part by the Whitaker Foundation and NIH grants CA-60711 and CA-54362.

[1]Local impulse response and local point spread function are used synonymously.

II. Background

The following approach is outlined for emission tomography, however, the method applies generally. Let $\underline{\lambda} = [\lambda_1, \ldots, \lambda_p]'$ represent the nonnegative emission rates for an object discretized into p pixels and lexicographically ordered, where $'$ denotes the Hermitian transpose. Projection measurements, $\underline{Y}$, of the object are obtained and are Poisson distributed with mean $\bar{Y}(\underline{\lambda}) = \boldsymbol{A}\underline{\lambda}$, where $\boldsymbol{A}$ is the system matrix.

Penalized-likelihood estimators often have the form

$$\hat{\underline{\lambda}}(\underline{Y}) = \arg\max_{\underline{\lambda}\in\Lambda} L(\underline{\lambda}, \underline{Y}) - \beta R(\underline{\lambda}),$$

where Λ is the set of feasible images, $L(\underline{\lambda}, \underline{Y})$ is the log-likelihood, β is the regularization parameter which controls the noise-resolution tradeoff, and $R(\underline{\lambda})$ is a roughness penalty. For our penalty design we choose a pairwise quadratic penalty, in which case the roughness penalty may be written in matrix form: $R(\underline{\lambda}) = \frac{1}{2}\underline{\lambda}'\boldsymbol{R}\underline{\lambda}$.

The tool by which we design the penalty and investigate the resolution properties of the estimator is the local impulse response. The local impulse response [1] at the jth pixel is defined as

$$\underline{l}^j \triangleq \lim_{\delta\to 0} \frac{\underline{\mu}(\underline{\lambda} + \delta\underline{e}^j) - \underline{\mu}(\underline{\lambda})}{\delta} = \frac{\partial}{\partial\lambda_j}\underline{\mu}(\underline{\lambda}),$$

where $\underline{\mu}(\underline{\lambda})$ is the mean reconstruction of the estimator and $\underline{e}^j$ represents the jth unit vector. This definition of the local impulse response is dependent on the estimator $\hat{\underline{\lambda}}$, the object $\underline{\lambda}$, and the pixel position j.

The matrix $\boldsymbol{A}$ can often be factored into $\boldsymbol{A} = D[c_i]\boldsymbol{G}$, where $\boldsymbol{G}'\boldsymbol{G}$ is nearly shift-invariant and diagonal matrix $D[c_i]$contains known ray-dependent effects such as detector efficiency and attenuation factors[2]. In this case, the local impulse response is approximately [1, 3]

$$\underline{l}^j \approx [\boldsymbol{G}'\boldsymbol{W}\boldsymbol{G} + \beta\boldsymbol{R}^{\text{sym}}]^{-1}\boldsymbol{G}'\boldsymbol{W}\boldsymbol{G}\underline{e}^j, \tag{1}$$

where $\boldsymbol{W} \triangleq D[c_i^2/\bar{Y}_i(\underline{\lambda})]$ and $\boldsymbol{R}^{\text{sym}} \triangleq \frac{1}{2}(\boldsymbol{R} + \boldsymbol{R}')$ is the symmetric component of $\boldsymbol{R}$.

III. Penalty Design Methods

A. Penalty Matrix Parameterization

Ideally, we would like to be able to find a penalty matrix $\boldsymbol{R}$ that yields an arbitrary desired space-invariant response.

[2]This factorization is often possible for PET systems.

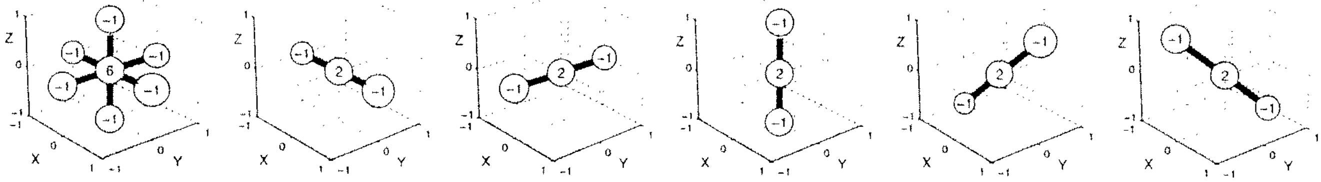

(a) k_{R_0} (b) $b_{(1,0,0)}$ (c) $b_{(0,1,0)}$ (d) $b_{(0,0,1)}$ (e) $b_{(1,0,1)}$ (f) $b_{(0,1,-1)}$

'ig. 1. Figure (a) shows a conventional shift-invariant "first-order" kernel, k_{R_0}. This kernel is an equivalent representation of the shift-invariant penalty matrix R_0. Figures (b-f) show several individual basis functions of the form given in (2). These functions are linearly combined to form arbitrary shift-invariant kernels, k_R, as given by (3). Thus we may parameterize arbitrary space-invariant penalty matrices, $\boldsymbol{R}$.

Iowever, since practical penalties use only a small neigh- orhood of pixels for the penalty support, we parameterize ? in terms of a small number of penalty coefficients.

For a shift-invariant quadratic penalty, the penalty ma- rix $\boldsymbol{R}$ can be thought of as a space-invariant filtering op- rator. Therefore the operation of multiplying $\boldsymbol{R}$ by the mage $\underline{\lambda}$ can be equivalently represented as the convolution f the image with a kernel[3],

$$\boldsymbol{R}\underline{\lambda} \equiv k_R * * * \underline{\lambda}.$$

'or example, a kernel for a conventional[4] "first-order" enalty is shown in Figure 1a. Thus, choosing a space- nvariant $\boldsymbol{R}$ can be thought of as filter selection.

Since the local impulse response (1) depends only on R^{sym}, we parameterize the kernel k_R in terms of a small umber of symmetric bases such as those having the fol- owing form

$$\begin{aligned} b_{(k,l,m)}(q,r,s) &= 2\delta(q,r,s) - \delta(q-k, r-l, s-m) \\ &\quad -\delta(q+k, r+l, s+m), \end{aligned} \tag{2}$$

here $\delta(\cdot)$ represents a Kronecker delta function, and q, , and s represent spatial coordinates. Several bases of his form are shown in Figure 1b-f. A collection of such $b_{(k,l,m)}(q,r,s)$ functions for various (k,l,m) triples can orm a basis for valid kernels of space-invariant $\boldsymbol{R}^{\mathrm{sym}}$ ma- rices. For example, for $\boldsymbol{R}^{\mathrm{sym}}$ with the same support as the ernel shown in Figure 1a, the set $\{b_{(1,0,0)}, b_{(0,1,0)}, b_{(0,0,1)}\}$ Figure 1b-d) forms a basis.

In general, any valid kernel for a space-invariant penalty atrix $\boldsymbol{R}^{\mathrm{sym}}$ may be specified by a linear combination of uch basis functions:

$$k_R = \sum_{k,l,m} r_{klm} b_{(k,l,m)} \equiv \boldsymbol{B}\underline{r} \tag{3}$$

here r_{klm} represent the basis coefficients. Let $\underline{r}$ represent he vector of all r_{klm} for a given neighborhood of support. f n_w is the number of (k,l,m) triples and hence the number f basis functions, then $\boldsymbol{B}$ is a $p \times n_w$ matrix with column vectors of lexicographically ordered basis functions, $b_{(k,l,m)}$. For nonnegative definite $\boldsymbol{R}^{\mathrm{sym}}$, the elements of $\underline{r}$ must be nonnegative.

[3]We use $\equiv$ since the left hand side is a vector but the right hand de is a 3D image. The two sides are equal in that the vector is a xicographic reordering of the 3D image.

[4]This kernel is most natural when there is equal sampling in all irections. However, such a kernel can be modified for nonuniform mpling.

As discussed in [1], space-invariant roughness penalties yield nonuniform resolution properties. For uniform reso- lution properties, we *require* a space-variant regularization. Therefore, we extend the kernel representation (3) and let $\boldsymbol{R}$ be parameterized by a space-variant set of coefficients $\underline{r}^j$, where j represents the jth pixel.

Let (q_j, r_j, s_j) denote the spatial coordinates of the jth pixel and define $\boldsymbol{B}^j$ to be a $p \times n_w$ matrix of shifted basis functions, with each column having elements defined by the lexicographically ordered bases, $b_{(k,l,m)}(q-q_j, r-r_j, s-s_j)$. In the case of a space-invariant $\boldsymbol{R}$ matrix, $\boldsymbol{R}\underline{e}^j = \boldsymbol{B}^j\underline{r}$. To parameterize space-variant $\boldsymbol{R}$, we define the jth column of $\boldsymbol{R}$ by

$$\boldsymbol{R}\underline{e}^j = \boldsymbol{B}^j\underline{r}^j, \quad j = 1, \ldots, p. \tag{4}$$

The parameterization (4) allows for the specification of valid shift-variant $\boldsymbol{R}^{\mathrm{sym}}$ by the set of coefficients $\{\underline{r}^j\}_{j=1}^p$.

B. Circulant Simplifications

Because the system matrix $\boldsymbol{A}$ is quite large, direct eval- uation of the local impulse response in (1) is not feasible. For a single pixel j, we may find $\underline{l}^j$ using iterative methods. However, this is not practical for penalty design.

Although $\boldsymbol{G}'\boldsymbol{W}\boldsymbol{G}$ is not globally shift-invariant, it is ap- proximately *locally* shift-invariant and we make the follow- ing approximation [7] to (1) using properties of circulant matrices

$$\underline{l}^j \approx \underline{l}^j_F(\boldsymbol{R}) \triangleq F^{-1}\left\{\frac{F\{\boldsymbol{G}'\boldsymbol{W}\boldsymbol{G}\underline{e}^j\}}{F\{\boldsymbol{G}'\boldsymbol{W}\boldsymbol{G}\underline{e}^j\} + \beta F\{\boldsymbol{R}^{\mathrm{sym}}\underline{e}^j\}}\right\}, \tag{5}$$

where the division is an element-by-element division and $F\{\cdot\}$ represents the discrete 3D Fourier operator.

Recalling (4), since local impulse responses are generally smoothly varying with location, $\boldsymbol{R}^{\mathrm{sym}}\underline{e}^j \approx \boldsymbol{B}^j\underline{r}^j$. Making this substitution in (5) gives us $\underline{l}^j(\underline{r}^j)$, the local impulse response in terms of the local penalty coefficients, $\underline{r}^j$. In principle, we may find the coefficients $\underline{r}^j$ by minimizing $\|\underline{l}^j(\underline{r}^j) - \underline{l}^j_0\|^2$, where $\underline{l}^j_0$ is a desired global response shifted to position j. This is a *nonlinear* least-squares minimization and appears impractical for routine use in penalty design, since it must be solved for $j = 1, \ldots, p$.

C. Linearized Penalty Design

Define $\underline{L}^j(\underline{r}^j) \triangleq F\{\underline{l}_F^j(\underline{r}^j)\}$ to be the frequency response of the local impulse response approximation $\underline{l}_F^j(\underline{r}^j)$ and let $\underline{L}_0 \triangleq F\{\underline{l}_0\}$ be the desired frequency response. We want to choose $\underline{r}^j$ so that $\underline{L}^j(\underline{r}^j) \approx \underline{L}_0$, *i.e.*

$$\underline{L}^j(\underline{r}^j) = \frac{F\{G'WG\underline{e}^j\}}{F\{G'WG\underline{e}^j\} + \beta F\{B^j\underline{r}^j\}} \approx \underline{L}_0. \quad (6)$$

Rearranging (6) by cross multiplying and simplifying yields

$$F\{G'WG\underline{e}^j\} \odot (1 - \underline{L}_0) \approx \underline{L}_0 \odot F\{\beta B^j \underline{r}^j\}, \quad (7)$$

where $\odot$ represents element-by-element multiplication. We can now design the penalty coefficients as a weighted least squares solution to (7). Specifically, we choose $\underline{r}^j$ such that

$$\hat{\underline{r}}^j = \arg\min_{\underline{r}^j \geq \underline{0}} \left\| \Phi^j \underline{r}^j - \underline{d}^j \right\|^2, \quad (8)$$

$$\Phi^j = VD[\underline{L}_0]F\{\beta B^j\} \quad (9)$$

$$\underline{d}^j = VD[1 - \underline{L}_0]F\{G'WG\underline{e}^j\}. \quad (10)$$

The matrix V is a least-squares weighting. This *linear* least-squares minimization may now be performed by using the NNLS (nonnegative least-squares) algorithm in [8].

D. Proposed Penalty Design

One natural choice for the desired impulse response is the unweighted response given by

$$\underline{l}_0 = [G'G + \beta R_0]^{-1} G'G\underline{e}^{j_0}, \quad (11)$$

where R_0 is a shift-invariant penalty.

Using the same simplifications for circulant matrices discussed previously to find an approximate $\underline{L}_0$, and choosing $V = D[F\{(G'G + \beta R_0)\underline{e}^{j_0}\}]$, we reduce (9) and (10) to

$$\Phi^j = D[F\{G'G\underline{e}^{j_0}\}]F\{B^j\} \quad (12)$$

$$\underline{d}^j = D[F\{k_{R_0}\}]F\{G'WG\underline{e}^j\}, \quad (13)$$

which are independent of β. Therefore, solving (8) using (12) and (13) yields the coefficients, $\{\hat{\underline{r}}_j\}_{j=1}^{P}$. These coefficients specify our proposed penalty matrix R^*, which provides for increased spatial uniformity.

IV. Simulation Results

To investigate the performance of this penalty design technique and to compare the resolution characteristics of a conventional shift-invariant penalty with our proposed penalty we consider the digital phantom presented in Figure 2. The emission image is $64 \times 64 \times 16$ with a warm background ellipse, a cold left disc, and hot right disc with relative emission intensities of 2, 1, and 3. The PET system model included nonuniform attenuation. Projections are obtained from a simulated system with 8 rings (covering -10 to 10 degrees off the XY plane) and 32 angles around the Z-axis.

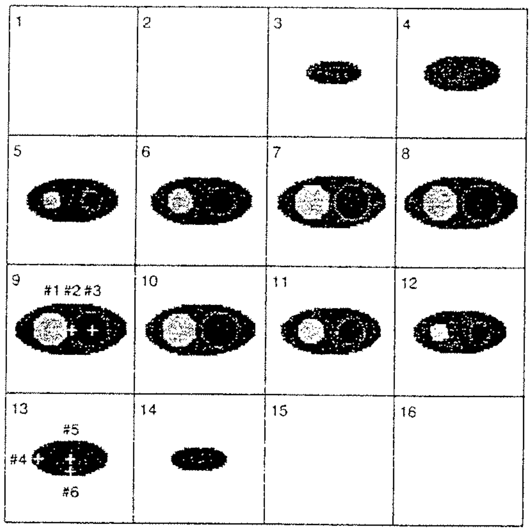

Fig. 2. Digital phantom used for investigation of resolution properties. The number in the upper left corner indicates the slice and the remaining numbers and white + marks indicate sample positions for local point spread function investigation.

For the conventional regularization we chose a smoothing kernel similar to the one in Figure 1a (but modified for Z sampling). For the proposed penalty, we used a computationally efficient implementation[5] of (8) using (12) with the basis set $\{b_{(1,0,0)}, b_{(0,1,0)}, b_{(1,1,0)}, b_{(1,-1,0)}, b_{(0,0,1)}, b_{(1,0,1)}, b_{(1,0,-1)}, b_{(0,1,1)}, b_{(0,1,-1)}\}$ and (13) with the same R_0 as in the conventional case.

To demonstrate the relative spatial uniformity of the conventional and the proposed penalties we used (1) to calculate local point spread functions (PSFs). Since shift-variant results are expected for the conventional regularization, we chose six different locations in the object for our investigation. These points are represented by the white + marks and are numbered #1 to #6 in Fig. 2.

Results of this impulse response survey are presented in Figures 3-4. For both penalties, PSF contours at 10, 25, 50, and 75% of peak value are shown. These contours cover three slices (*i.e.*: one local PSF has contours in three planes). Conventional results are shown in the left group and the proposed penalty is shown in the right group.

For the conventional penalty there is greater smoothing in the hot region (#3) and less smoothing in the cold region (#1). The smoothing is also anisotropic, all of the PSFs smooth more in the Y direction than in the X direction. There is also asymmetric smoothing in Z for #4-#6.

For the proposed penalty, the PSF contours tend to be much more radially symmetric in the XY plane and overall are much more spatially uniform. (The PSFs in the right group are very similar.) The asymmetries in the Z direction are also much improved. (More improvement may be possible with a larger penalty support. Note, bases such as $b_{(1,1,1)}$ were not used.)

[5]The computationally efficient method used here is an extension of the methods used in the 2D case presented in [3],

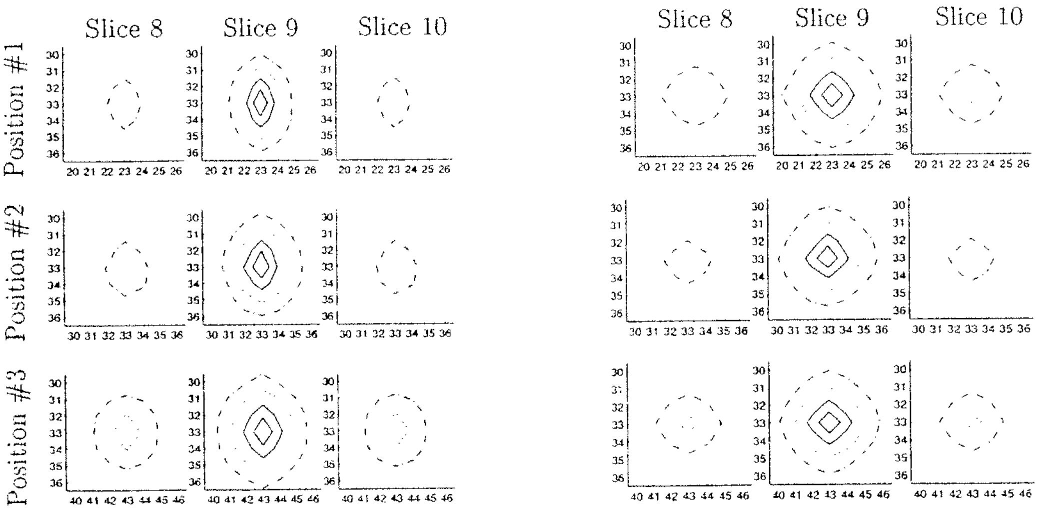

Fig. 3. Local PSFs for conventional penalty (left group) and for the proposed penalty (right group) for positions #1 - #3 in slice 9.

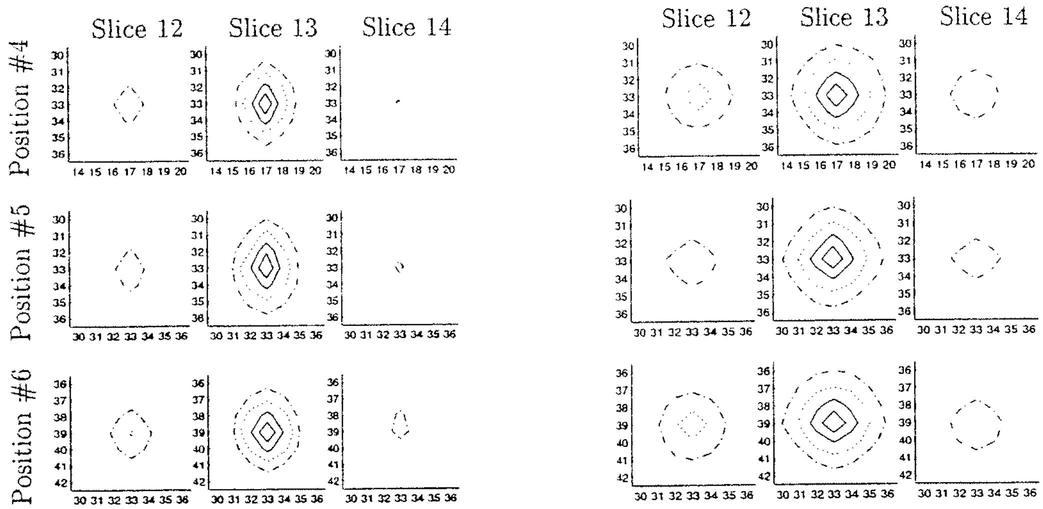

Fig. 4. Local PSFs for conventional penalty (left group) and for the proposed penalty (right group) for positions #4 - #6 in slice 13.

V. Discussion

Conventional space-invariant regularization methods for penalized-likelihood image reconstruction produce images with space-variant resolution properties. We have presented a new regularization scheme for increased spatial uniformity. The proposed method is based on fitting a parameterized local impulse response to a desired response. This method yields nearly space-invariant and nearly symmetric local point spread functions.

The importance of uniform resolution is an open question. Having uniform resolution is logical for cross-patient or multiple-image single patient studies, or for comparing resolution matched reconstruction methods. Although one may arguably desire space-variant resolution properties, one would most likely want to be able to control regional resolution properties. The proposed methods can be modified to provide such control, allowing for predictable and intuitive specification of resolution properties.

This paper concentrates on the resolution (bias) properties of different estimators, future work will include a variance investigation. These local impulse response studies suggest improved resolution uniformity, however reconstructions on real data must also be performed.

References

[1] J. A. Fessler and W. L. Rogers, "Spatial resolution properties of penalized-likelihood image reconstruction methods: Space-invariant tomographs," *IEEE Tr. Im. Proc.*, vol. 5, pp. 1346–58, Sept. 1996.

[2] J. A. Fessler, "Resolution properties of regularized image reconstruction methods," Tech. Rep. 297, Comm. and Sign. Proc. Lab., Dept. of EECS, Univ. of Michigan, Ann Arbor, MI, 48109-2122, Aug. 1995.

[3] J. W. Stayman and J. A. Fessler, "Regularization for uniform spatial resolution properties in penalized-likelihood image reconstruction," *IEEE Tr. Med. Im.*, 1998. Submitted.

[4] J. W. Stayman and J. A. Fessler, "Spatially-variant roughness penalty design for uniform resolution in penalized-likelihood image reconstruction," in *Proc. IEEE Intl. Conf. on Image Processing*, 1998.

[5] D. W. Wilson and B. M. W. Tsui, "Spatial resolution properties of FB and ML-EM reconstruction methods," in *Proc. IEEE Nuc. Sci. Symp. Med. Im. Conf.*, vol. 2, pp. 1189–1193, 1993.

[6] C. Comtat, P. E. Kinahan, M. Defrise, C. Michel, and D. W. Townsend, "Fast reconstruction of 3D PET data with accurate statistical modeling," *IEEE Tr. Nuc. Sci.*, vol. 45, pp. 1083–9, June 1998.

[7] J. A. Fessler and S. D. Booth, "Conjugate-gradient preconditioning methods for shift-variant PET image reconstruction," *IEEE Tr. Im. Proc.*, 1997. To appear.

[8] C. L. Lawson and R. J. Hanson, *Solving least squares problems*. Prentice-Hall, 1974.